FLEXIBLE POLYIMIDE AEROGELS DERIVED FROM USE OF NEOPENTYL SPACER IN BACKBONE

Jessica L. Cashman[1*], Baochau N. Nguyen[2*], Bushara Dosa[1], Mary Ann B. Meador[1]

1. NASA Glenn Research Center, 21000 Brookpark Road, Cleveland OH 44135

2. Ohio Aerospace Institute, 22800 Cedar Point Road, Brookpark, OH 44142

[*] Corresponding author: jessica.l.cashman@nasa.gov, baochau.n.nguyen@nasa.gov

RECEIVED DATE (to be automatically inserted after your manuscript is accepted if required according to the journal that you are submitting your paper to)

TITLE RUNNING HEAD: Flexible polyimide aerogels.

ABSTRACT Polyimide aerogels have gained much attention in the last decade due to their highly porous structure with low density, low dielectric constant, good mechanical properties and thermal stability. They are desirable for many aerospace and commercial applications including lightweight substrates for antennas for aerospace vehicles, due to the low dielectric constant, approaching one as density decreases. However, with only aromatic diamines in the backbone, the aerogels are flexible only as very thin films, nominally 0.5 mm thick. A more flexible aerogel

substrate would allow them to be used as conformal antennas, which would reduce drag and also save space in aerospace vehicles. In this research, we demonstrate that the flexibility can be increased by substituting the aromatic diamines typically used in polyimide aerogels with 1,3-bis(4-aminophenoxy)-2, 2-dimethylpropane (BAPN), which contains a flexible neopentyl spacer group. Using the aliphatic diamine, BAPN, leads to aerogels with a high bend radius even when the aerogels are 2-3 mm thick. Twenty different formulations of polyimide aerogels were synthesized from 3,3',4,4'-biphenyltetracarboxylic dianhydride (BPDA) and a combination of BAPN and 2,2'-dimethylbenxidine (DMBZ), and cross-linked with 1,3,5-triaminophenoxybenzene (TAB) to understand the effect of polymer concentration, oligomer chain length and concentration of BAPN on the properties of the aerogels. Aerogels made using 50 mol % BAPN with n of 45 and 7 wt % polymer possessed the best combination of properties conducive to use as a flexible substrate for conformal antennas, including low density, good hydrophobicity, low shrinkage with high surface area, a one-inch bend radius in aerogels up to 3 mm thickness, and a dielectric constant of 1.11.

Key words: polyimide aerogels, dielectric constant, hydrophobic, mesoporous, surface area

Introduction

Aerogels are extremely porous materials made by extracting the liquid portion of a wet gel and replacing it with air. This light weight, nanoporous architecture[1] is preserved through supercritical fluid extraction or other methods to minimize shrinkage.[2, 3, 4] Because of the way they are made, aerogels have extremely low densities, and high surface areas. These properties result in materials with very low thermal and electrical conductivities[5]. While polyimides with fluorinated substitution, for example, have been shown to have lower dielectric constants,[6, 7, 8] we have

previously demonstrated that polyimide aerogels even with varying amounts of fluorination in the backbone are dependent only on density[9], approaching one as density decreases.[10, 11]

Aerogels have been made using many different backbones, including silica[12, 13, 14] and other ceramics[15, 16], ceramic polymer hybrids[17, 18], and polymers.[19, 20, 21] Silica aerogels have been the most extensively studied and have extremely high surface areas, low thermal conductivities, and low dielectric constants, but are typically very brittle and moisture sensitive. Polymer aerogels not only maintain the desirable physical properties that silica aerogels offer, but also have far superior mechanical properties.[22, 23] Among polymer aerogels, polyimide aerogels are notable, as they combine increased durability as well as higher temperature stability,[24,25] making them suitable for many aerospace applications, including insulation for launch vehicles or aircraft, [11, 26] and low dielectric substrates for devices such as antennas.[10, 27]

Antennas made using low dielectric substrates exhibit reduced radio frequency losses, improved impedance matching, higher gain, and wider bandwidth. Polyimide aerogels possess low dielectric constants that vary linearly with density.[9, 28] Patch antennas were recently demonstrated using an aerogel with a dielectric constant of 1.16.[11, 29] Compared to those made using commercial fiberglass and fluorocarbon composite substrates with a dielectric constant of 2.2, the aerogel antennas showed very promising results, with higher gain across a wider frequency range and more than a 75 % weight reduction.[11, 29] The aerogel substrates were also demonstrated in eight and 32 element antenna arrays, indicating that the technology is scalable.[29]

Typically, antennas used in large unmanned air vehicles (UAV) and other large aircraft are dish antennas which are pointed using a gimbal. These take up a huge amount of space and are too heavy to use in smaller aircraft and UAV. Conformal phased array antennas can result in enormous space and weight savings, and may allow smaller UAV to communicate with satellites, enabling

beyond line of sight command and control. This is due not only to greatly reducing the physical mass of the antenna, but also to eliminating drag, furthering the weight savings.[30, 31]

To enable an antenna to conform to a surface, the aerogel substrate must be flexible. All aromatic polyimide aerogels are flexible only as thin films, approximately 0.5 mm thick.[32] This is because the stiffness of polyimide aerogels primarily depends on backbone chemistry.[33] Thus, the inherent molecular rigidity of the aromatic diamines and dianhydrides, results in a rigid aerogel—unless the aerogel is very thin. On the other hand, aerogels with all aliphatic diamines result in higher shrinkages and densities and smaller surface areas[34], therefore, leading us to consider a backbone that has both aliphatic and aromatic groups.

We have previously demonstrated that by incorporating diamines with aliphatic spacers in the backbone of the polyimide, flexible aerogels can be produced with large bend radii at thicknesses of up to 2-3 mm[35], which to the best of our knowledge is the first example of this, though it is worth noting that flexible aerogels of comparable thicknesses have been developed from polyurethanes[36, 37, 38, 39]. In the flexible polyimide work, a diamine containing aliphatic spacers of three different lengths were examined. The diamines 1,4-bis(4-aminophenoxy)butane (BAP4), 1,6-bis(4-aminophenoxy)hexane (BAP6), or 1,10-bis(4-aminophenoxy)decane (BAP10), with either four, six, or ten methylenes in the spacer, more generally referred to as BAPx, were used in conjunction with the diamine, 2,2'-dimethylbenxidine (DMBZ). The dianhydride used was 3,3',4,4'-biphenyltetracarboxylic dianhydride (BPDA), and 1,3,5-triaminophenoxybenzene (TAB) was used as the cross-linker. The result from the study was that formulations made using at least 25 mol % BAPx all resulted in more flexible aerogels. Mechanical properties, density and dielectric constant depended less on the length of the spacer and more on the amount of flexible spacer used, while BAP10 had better moisture resistance.[35]

To build on this work, we wish to examine the effect of substituting up to 75 mol % of DMBZ with, 1, 3-bis (4-aminophenoxy)-2, 2-dimethylpropane (BAPN), which has a shorter branched neopentyl spacer. We will compare the properties of aerogels using this spacer to the linear spacers previously studied. As in the previous study, the aerogels were fabricated as shown in Scheme 1 using BPDA as the dianhydride, with TAB as the cross-linker. In addition, the total polymer concentration was varied between 7, 8.5, and 10 wt %, and the formulated number of repeat units, n, was varied between 30, 45, and 60. A statistical design of experiment was used to evaluate the effect of these variables on density, dielectric constant, water resistance, and mechanical properties, with a focus on flexibility.

Scheme 1. Synthesis of BAPN-containing polyimide aerogels

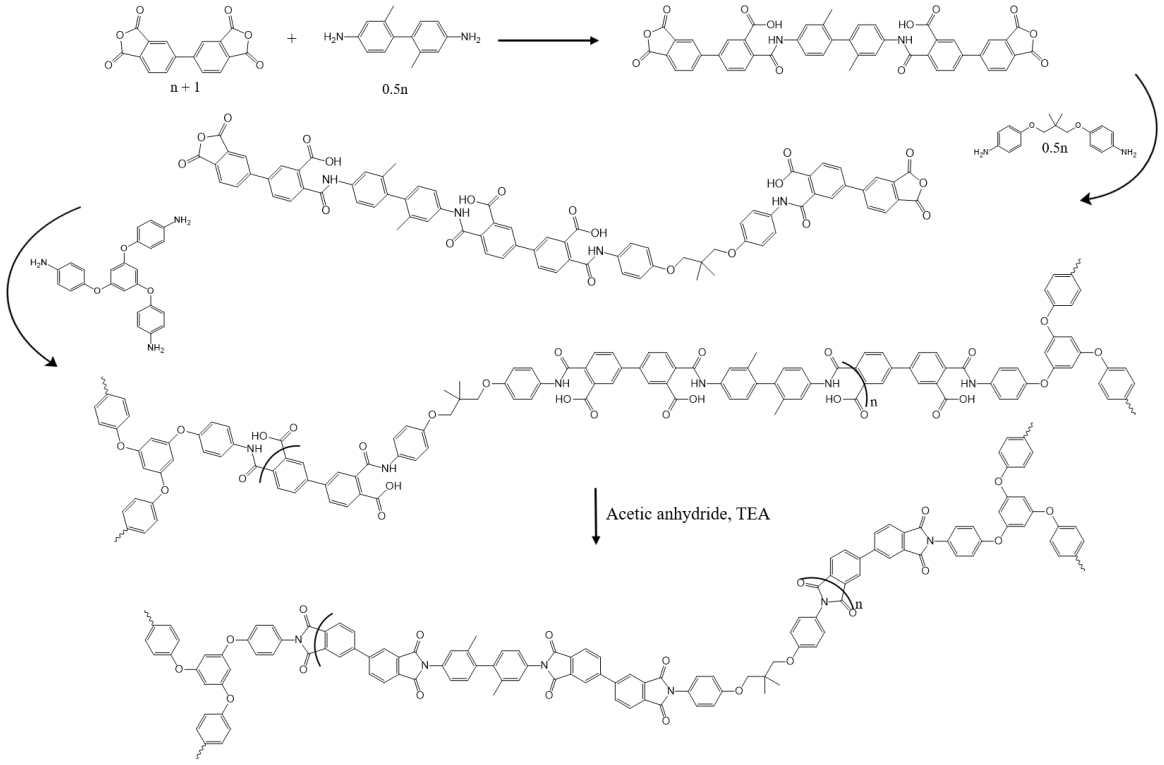

Experimental Procedures

Materials. Acetic anhydride (≥ 98%) (AA), and trimethylamine (≥ 99%) (TEA) were purchased from Sigma-Aldrich®. Acetone (≥ 99.5%) was purchased from Fisher Chemical and N-methyl-2-pyrrolidinone (99.5%) (NMP) was purchased form Tedia®. 2,2'-Dimethylbenzidine (DMBZ) was purchased from Wakayama Seika Kogyo Co., Ltd., 1, 3-bis (4-aminophenoxy)-2, 2-dimethylpropane (BAPN) from TCI America, and biphenyl-3,3',4,4'-tetracarboxylic dianhydride (BPDA) were obtained from UBE America, Ltd. and 1,3,5-triaminophenoxybenzene (TAB) was purchased from Triton Systems Deionized water was prepared using a reverse osmosis desalination system. All other reagents were used without further purification.

General. The gels were dried and the bulk densities, skeletal densities, percent porosity, percent shrinkage, and Brunauer-Emmett-Teller (BET) were calculated according to the procedure in Nguyen et al.[40] Thermal gravimetric analysis (TGA), ^{13}C solid-state nuclear magnetic resonance (NMR) spectroscopy, attenuated total reflectance (ATR) infrared spectroscopy, and scanning electron microscopy (SEM) images were performed and collected according to the procedure in Pantoja et al.[35]

Synthesis of BAPN-Containing Polyimide Aerogels. Polyimide gels were synthesized according to Scheme 1 using the dianhydride, BPDA, and the diamines, BAPN and DMBZ. As an example, the procedure for the synthesis of sample 1, from Table 1 consisting of 50 mol % BAPN, n = 45, and a polymer concentration of 8.5 wt % is as follows:

On a hot plate that was set to a nominal 40 °C, BPDA (2.45 g, 8.34 mmol) was added to a solution of DMBZ (0.87 g, 4.08 mmol) and 42 mL of NMP to form short anhydride capped oligomers. Once all of the DMBZ and BPDA dissolved, BAPN (1.17 g, 4.08 mmol) was added to chain extend the short oligomers and form mostly alternating copolymers with anhydride endcaps. After BAPN

dissolved, a solution of TAB (0.0610 g, 0.121 mmol) dissolved in 2.5 mL of NMP was added to cross-link the poly (amic) acid, forming a three-dimensional structure. Once the solution became homogenous, acetic anhydride (6.31 mL, 66.7 mmol, 8:1 molar ratio relative to BPDA), a water scavenger, followed by triethylamine (2.33 mL, 16.7 mmol, 2:1 molar ratio relative to BPDA), a base catalyst used to catalyze the imidization, was added. The solution was stirred for an additional 5 minutes and then poured into various molds and covered with parafilm to avoid solvent evaporation. These molds included a 20 mL syringe mold prepared by cutting off the needle end and extending the plunger all the way out, a dog bone silicone mold, and a rectangular closed mold (nominally 2.4 mm x 25 cm x 18 cm). The rectangular mold is made of stainless steel panels that connect via screws. Stainless steel spacers are added to adjust the thickness of the mold. The inside of the mold was coated with a non-stick dry film lubricant to facilitate the demolding of the sheet samples. Gelation occurred within 40 minutes depending on the formulation. The gels were then left to age overnight in the molds at room temperature before being extracted into a bath of NMP.

The NMP in the wet gels was gradually replaced by acetone through solvent exchange. The gels were first soaked in 50 v/v % NMP in acetone, then only acetone, followed by four more immersions in pure acetone in half day increments. The gels were converted into aerogels using supercritical CO_2 extraction, followed by outgassing in a vacuum oven at 80 ^{o}C overnight to remove any residual solvent before being characterized and tested. The resulting aerogel had a density of 0.119 g/cm^3, a shrinkage of 15 %, was 92 % porous, and had a BET surface area of 305 m^2/g. ^{13}C solid-state NMR (ppm): 166, 158, 144, 131, 124, 67, 26 and 19. FT-IR (cm^{-1}): 2975-2840 (alkane), 1774, 1719, 1372 (imides), 1613 and 1490 (C=C stretch), 1248 and 1117 (ether C-O-C stretch diaryl), 1300, 1175 and 1091 (C-O-C stretch dialkyl), 828, 739 cm^{-1}.

Table 1. Formulations and properties of DMBZ/BAPN- containing polyimide aerogels

Sample	Polymer Conc. (wt %)	Repeat Units, n	BAPN (mol %)	Bulk Density (g/cm^3)	Porosity (%)	Shrinkage (%)	BET Surface Area (m^2/g)	Modulus Compression (MPa)	Modulus 3- Point bend (MPa)	Modulus Tensile (MPa)	Dielectric Constant	Water Uptake (g/cm^2)
1	8.5	45	50	0.119	92	15	305	15.2	34.4	39.3	1.15	*
2	8.5	45	50	0.117	92	14	258	*	36.0	33.7	1.15	1.5E-03
3	8.5	45	75	0.251	83	30	268	89.1	66.2	57.9	1.21	1.1E-02
4	8.5	45	50	0.119	91	15	318	24.5	36.8	37.2	1.16	1.6E-03
5	7	30	75	0.162	89	28	256	13.9	18.1	18.6	1.18	3.7E-03
6	10	45	50	0.128	91	13	401	44.2	44.4	56.6	1.17	3.4E-03
7	8.5	45	50	0.106	93	11	378	19.3	22.9	27.3	1.14	1.4E-03
8	10	60	75	0.304	78	35	259	*	127.3	228.3	*	1.4E-02
9	7	60	75	0.166	88	28	239	13.1	32.5	27.2	1.18	4.1E-03
10	8.5	45	25	0.118	92	15	390	31.3	39.2	45.6	1.14	3.2E-03
11	7	60	25	0.094	94	14	438	*	26.2	24.0	1.12	2.3E-01
12	7	45	50	0.079	95	9	424	10.1	14.2	40.8	1.11	1.6E-03
13	10	30	75	0.236	83	29	253	139.9	87.6	91.0	1.26	1.9E-02
14	10	30	25	0.121	91	12	458	43.7	49.3	45.4	1.20	2.1E-03
15	8.5	60	50	0.131	90	18	286	10.8	33.3	43.5	1.15	2.4E-03
16	8.5	45	50	0.109	92	12	372	17.0	28.3	37.7	1.15	1.5E-03
17	8.5	30	50	0.119	92	15	323	26.3	35.9	35.2	1.15	2.7E-03
18	10	60	25	0.157	89	19	392	25.0	77.9	74.7	1.21	5.1E-03
19	7	30	25	0.096	93	13	490	10.5	*	19.2	1.11	4.8E-03
20	8.5	45	50	0.102	93	11	358	16.9	22.4	62.8	1.13	1.3E-03

*not measured.

Dielectric Constant Measurements. Dielectric constant was measured using a Keysight 85072A 10-GHz Split Cylinder Resonator, analysis was done using algorithms developed at National Institute of Standards and Technology's (NIST) Electromagnetics Division in Boulder, Colorado[41, 42] and the procedure described in Pantoja et al.[35] was followed.

Compression Testing. Cylindrical samples, nominally 16.2 mm in diameter by 21.1 mm in length, were used for compression testing, based on ASTM standard D695-10 and followed the

preparation and testing method described in Pantoja et al.[35] The data acquisition systems used were an Aramis GOM 3D Optical Measuring System and an MTS TestWorks 4.0.

Tensile Testing. Dog bone specimens, nominally 5.2 mm wide and 4.9 mm thick, were tested according to ASTM D882 and followed the procedure described in Pantoja et al.[35] The strain measurement program used was a GOM Aramis v6.3.1.

Three-Point Bending. Rectangular samples 10.2 mm long x 8.3 mm wide x nominally 1.8 mm thick, were tested according to ASTM D790-15 using a TA Instruments Q800 dynamic mechanical analysis (DMA), a commonly used instrument for three-point bending tests that does not require a large sample for testing. The procedure was performed according to the one described in Pantoja et al.[35]

Water Uptake. Rectangular samples nominally 2.9 cm x 2.0 cm x 0.9 cm were tested according to ASTM D570-98 and followed the procedure as described in Pantoja et al.[35]

Statistical analyses. Design Expert 9 software from Stat-Ease, Inc., was used to generate a set of 20 experiments with a face-centered central composite design. The design included five repeats of the center point for reliability and accuracy. The variables included were: 1) concentration of polyimide in NMP, ranging from 7 to 10 wt %; 2) the formulated number of repeat units, n, of the oligomer from 30 to 60; and 3) the concentration of BAPN used as a mol percent of the total diamine used, ranging between 25 – 75 mol %, with the balance being DMBZ. Insignificant terms ($p < 0.1$) were removed from the model one at a time, using backward stepwise regression.

Results and Discussion

Aerogels made according to Scheme 1 using the variables listed in Table 1 were analyzed by solid-state ^{13}C NMR. ^{13}C solid-state NMR spectra of runs #3 (75 mol % BAPN), #16 (50 mol % BAPN) and #10 (25 mol % BAPN) are shown in Figure 1. The intensity of all three spectra was normalized

at 166 ppm. The NMR spectra of all the samples analyzed contain an imide carbonyl peak (1) at 166 pm.[43] The peak at 158 ppm (2) belongs to the aromatic ether carbons from the BAPN.[44] The peak at 144 ppm (3) corresponds to the aromatic carbons in the biphenyl link of BPDA. Broad peaks ranging from 130 ppm to 110 ppm are assigned to other aromatic carbons on BPDA, DMBZ and BAPN. The aliphatic ether carbon of BAPN appears at 67 ppm (4) and methyl groups of BAPN appear at 26 ppm (5). The methyl groups of DMBZ appear at 19 ppm (6). The intensities of peaks 2, 4 and 5 increase as the amount of BAPN increases while the DMBZ peak 6 decreases.

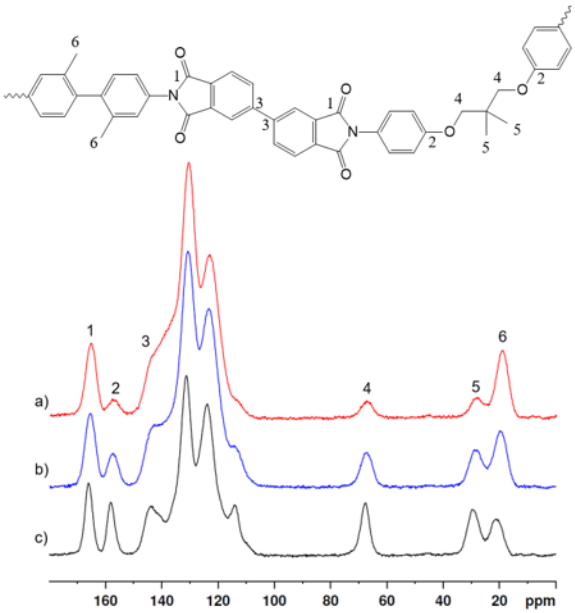

Figure 1. ^{13}C solid-state NMR spectra of polyimide aerogels with a) 25 mol % BAPN, b) 50 mol % BAPN, and c) 75 mol % BAPN

Figure 2 shows FT-IR spectra of runs # 3 (75 mol % BAPN), #16 (50 mol % BAPN) and # 10 (25 mol % BAPN). Imide rings peaks appear at wavenumbers of 1775 cm^{-1} and 1721 cm^{-1} due to C=O stretching of imide. The absence of peaks due to unreacted anhydride, amic acid (C = O), and amide (C – N) at 1860 cm^{-1}, 1660 cm^{-1} and 1535 cm^{-1}, respectively, indicate complete imidization. The peaks at 1614 cm^{-1} and 1510 cm^{-1} are the C=C stretch from the aromatic rings in both diamines. The peak at 1367 cm^{-1} comes from both the C-N stretch from the polyimide ring

and the CH bend from the methyl group from BAPN, overlapping each other. The peak around 3050 cm^{-1} is the CH stretch of CH_3 from DMBZ. As for BAPN, peaks from 2931cm^{-1} – 2854 cm^{-1} are assigned to the CH stretch of alkanes from BAPN. The peaks at 1247 cm^{-1}, 1175 cm^{-1} and 1093 cm^{-1} are characteristic of C-O-C stretch (alkyl and aryl). The intensity of all three spectra was normalized at 1721 cm^{-1}. Similar to what was observed in NMR spectra, the intensity of peaks related to BAPN, 1367 cm^{-1}, 1247 cm^{-1}, and 2931cm^{-1} – 2854 cm^{-1}, increases in formulations derived from higher BAPN concentrations.

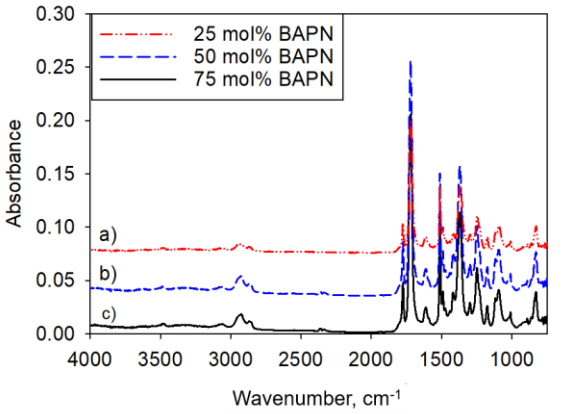

Figure 2. FT-IR spectra of polyimide aerogels: a) 25 mol % BAPN, b) 50 mol % BAPN and c) 75 mol % BAPN

The data in Table 1 was analyzed using multiple linear regression to derive empirical models which show the effect of the three variables studied on the measured responses. Figure 3 shows empirical models for a) diametrical shrinkage (standard deviation = 1.51 %, R^2 = 0.98) and b) density (standard deviation = 0.0115 g/cm^3, R^2 = 0.98) of the aerogels vs. total polymer concentration and BAPN concentration at three levels of n. Increasing concentration of BAPN significantly increases shrinkage (Figure 3a), especially when BAPN concentration is above 50 mol %. The second order effect may be due to the order of addition of the diamines, and the ratio of diamine and BPDA present at each step of the reaction. Scheme 1 shows that 25 to 75 mol %

DMBZ was first reacted with all the BPDA. When the amount of DMBZ was 50 mol %, the predominant oligomer in solution in the first step of the synthesis would thus be the n = 1 oligomer, BPDA-DMBZ-BPDA since BPDA is present in a two to one excess. Thus, addition of BAPN should result in an oligomer with an alternating structure. While it would be difficult to prove that an alternating structure is formed, it has been observed in a previous study where two diamines are used that different morphologies are produced based on order of addition.[45] In that study, reacting 4,4'-oxidianiline (ODA) and DMBZ together with BPDA results in aerogels with hierarchical structures and poorer mechanical properties, while reacting the ODA with all of the BPDA and then adding DMBZ resulted in more homogeneous structures. The only logical explanation is that the former results in random copolymers which can phase separate during gelation, while in the latter, alternating copolymers are formed which cannot phase separate.

When DMBZ concentration is 75 mol %, the ratio of BAPN to BPDA is about three to four which would result in predominantly n = 3 oligomers terminated with BPDA. Addition of 25 mol % BAPN would still result in oligomers where the BAPN is isolated from one another along the chain. Starting with only 25 mol % DMBZ in solution would result in n = 1 oligomers but also an excess of unreacted BPDA. Addition of 75 mol % BAPN would then result in oligomers with longer runs of BAPN-BPDA, unseparated by the more rigid DMBZ-BPDA segments. Thus, aerogels made using 75 mol % BAPN may experience a much higher shrinkage, associated with the increased flexibility of the aliphatic linkages, and possibly more pore collapse. The same increase in shrinkage was also observed in the previously reported study using BAPx as the aliphatic spacer diamine.[35] Indeed, the shrinkage using 75 mol % BAPN is about 30 to 35 %, very similar to those aerogels made using 75 mol % BAPx. At lower concentrations of BAPN, the shrinkage was less than that seen in the BAPx study, possibly due to the effect of the branched

structure in BAPN. The shrinkage also increases with increasing polymer concentration, particularly when n = 60, as there are less cross-link sites in the three-dimensional structure.

Density mainly depends on polymer concentration (which affects the mass) and shrinkage (which affects the volume). Hence, in Figure 3b, as polymer concentration is increased, the density increases as well. Due to the synergistic effect of polymer concentration and number of repeat units on shrinkage, density also increases more as polymer concentration is increased, especially at n = 60. The density also increases with increasing BAPN concentration, due to the increase in shrinkage. Hence, the highest density aerogels are those made using the highest number of repeat units with the highest concentration of polymer and BAPN. There is only a small difference in the density of samples made using 25 and 50 mol % BAPN, with aerogel densities 0.157 g/cm^3 and below across the design space. As with shrinkage, similar densities were seen for aerogels made using BAPx in the previous study.[35]

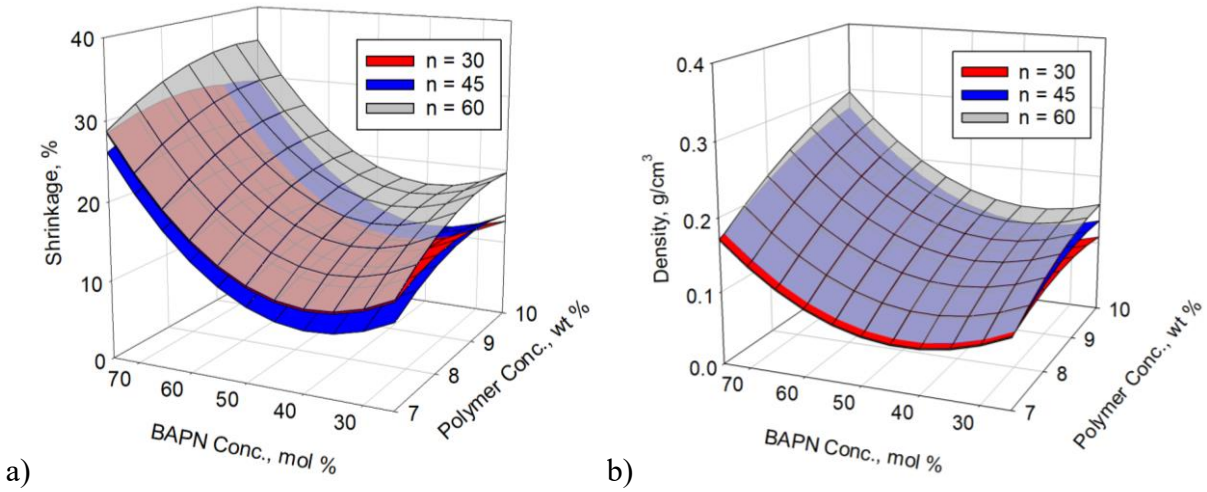

Figure 3. Empirical model for a) shrinkage of aerogels, and b) density of aerogels at different n's vs. total polymer concentration and BAPN concentrations.

Scanning electron micrographs (SEM) of representative formulations are shown in Figure 4. Formulations made using 7 wt % polymer concentration, n = 60, and 25 mol % BAPN (Figure 4a, b) and 75 mol % BAPN (Figure 4c, d), are shown at low and high magnifications. The morphology for aerogels formulated with BAPN concentrations of 50 mol % are similar to those at 25 mol %, in agreement with the findings for shrinkage. The SEM images at low magnification (4a and 4c) show difference in pore structure from 25 mol % to 75 mol % BAPN. The fibrils of the aerogels derived from lower concentrations of BAPN are much finer than those derived from higher BAPN concentrations, which is the same trend seen in aerogels made with 25 and 75 mol % BAP10.[35] This coarsening of the fibrils with increasing BAPN is even more pronounced in Figure 4 e-h where the polymer concentration is 10 wt %, n = 60, and 25 mol % BAPN (Figure 4e, f) and 75 mol % BAPN (Figure 4g, h). The extreme is shown in Figure 4g, which shows micron sized struts that upon further magnification (Figure 4h) are comprised for coarse nano-sized fibrils. Additionally, when comparing the microstructure of aerogels derived from the same amounts of BAPN, the aerogels made at higher polymer concentrations appear to have more densely packed fibrils, which is expected since density increases with increasing polymer concentration.

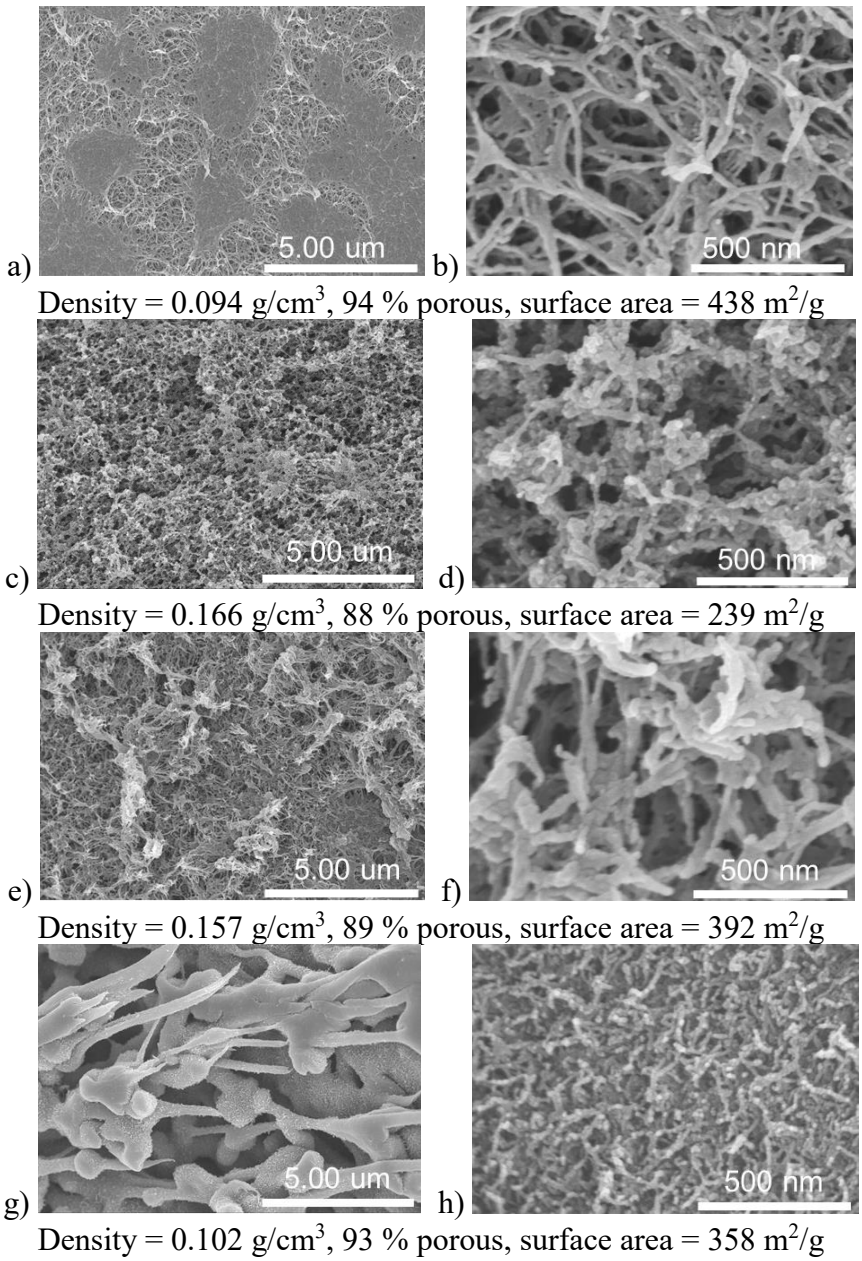

Figure 4. Low (left) and high (right) magnification SEM micrographs of aerogels made using 7 wt % polymer concentration, n = 60, and a) and b) 25 mol % BAPN, c) and d) 75 mol % BAPN; Aerogels made using 10 wt % polymer concentration, n = 60, and e) and f) 25 mol % BAPN, and g) and h) 75 mol % BAPN

Surface area is measured using nitrogen sorption and analyzed using Brunauer Emmet Teller (BET) method.[46] Figure 5a shows the empirical model for the BET surface area vs. BAPN

concentration and polymer concentration, at three levels of n (standard deviation = 34.57 m^2/g, R^2 = 0.85). Surface area decreases linearly with increasing BAPN concentration, similar to the previous study using BAPx[35] instead of BAPN. This is due to the decrease in mesopore volume as shown in Figure 5b, which plots the pore volume vs. pore diameter for aerogels made using different amounts of BAPN. Increasing polymer concentration leads to a slight parabolic effect, where 8.5 wt % shows the smallest surface area. Additionally, n has a small second order effect on the surface area is highest with samples made with n = 45 with n = 60 having the lowest surface area.

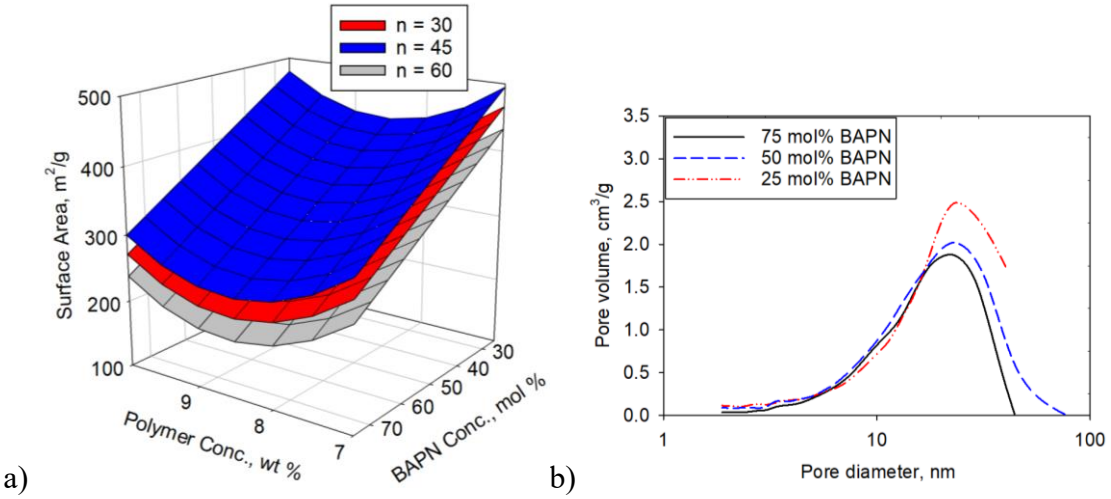

Figure 5. a) Empirical Model for BET surface area and b) Plot of pore size distribution

Figure 6 shows that the dielectric constant increases linearly with increasing density (standard deviation = 0.0065, R^2 = 0.99), which has been seen in previous studies.[28, 35] The sample with the lowest density, made using 7 wt % polymer, n = 45, and 50 mol % BAPN, has the lowest dielectric constant, 1.109, but all samples produced in the study have substantially lower dielectric constants than substrates used currently in conventional antennas, which have dielectric constants of approximately 2.2.[11, 29]

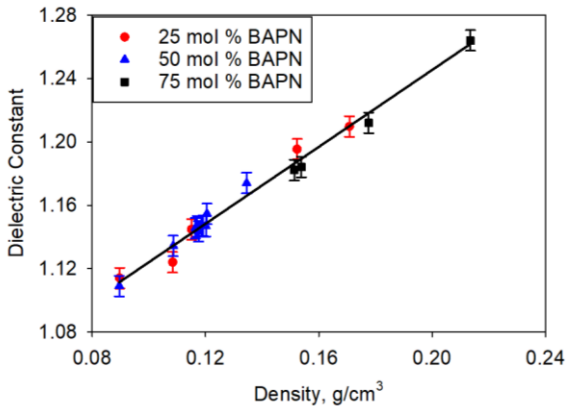

Figure 6. Graph of dielectric constants vs. density for aerogels in the study.

The thermal stability of polyimide aerogels derived from BAPN is seen in Figure 7, which shows thermal gravimetric analysis (TGA) of aerogels derived from 25, 50, and 75 mol % BAPN in a nitrogen environment. There is no significant weight loss around 200 ºC, indicating complete imidization, which is consistent with the findings in FT-IR. It can be seen that the onset of decomposition happens at about 435 ºC for samples derived from 75 mol % BAPN. Samples derived from 25 and 50 mol % BAPN show onset of decomposition at about 450 ºC. For comparison, the onset of decomposition for aerogels made using only DMBZ with BPDA and TAB is about 511 ºC[32], and the onset of decomposition for samples in the BAPx study range from approximately 475 – 510 ºC[35]. Polyimides made using BAPN and benzophenone-3,3',4,4'-tetra-carboxylic dianhydride (BTDA) have a thermal decomposition temperature of 400 ºC[47]. Aerogels made with DMBZ and BTDA have a thermal decomposition temperature of 470 ºC[32], indicating the lower decomposition temperature of polyimides with BAPN and BTDA is due to the aliphatic portion of BAPN. As expected, the aerogels in this study have thermal decomposition temperatures between the lower limit of BAPN, 400 ºC, and the upper limit of all DMBZ aerogels, 511 ºC. It is expected that the onset of thermal degradation would be lower for samples containing more aliphatic linkages, since aliphatic linkages are less thermally stable than fully aromatic ones. The

second drop in the TGA curve occurs where the onset of decomposition typically is seen in polyimides with no aliphatic links. The difference in char yield is also related to the amount of aliphatic linkages, where aerogels made using 75 mol % BAPN experience the most weight loss, followed by 50 mol % and 25 mol % BAPN, as expected.

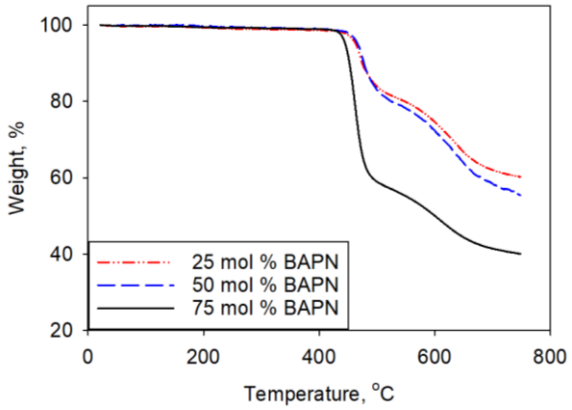

Figure 7. TGA of samples made with 25, 50, and 75 mol% BAPN in a nitrogen environment

Figure 8a shows compressive stress-strain curves for selected aerogel formulations at 10 wt % polymer concentration and varying amounts of BAPN. The Young's Modulus is obtained by taking the slope of the linear portion of the stress-strain curve. The linear portion of the curve is the elastic deformation region, followed by yielding and the plastic deformation region. The entire curve is not shown here, as the test was stopped after about 5 % strain was reached rather than compressive failure. The initial rise of the curve is highest when the concentration of BAPN is 75 mol %. The initial rise for samples with 50 and 25 mol % BAPN is similar. The sample with 75 mol % BAPN begins to yield at a lower % stress than the samples derived from 50 and 25 mol % BAPN.

The empirical model in Figure 8b shows the compressive log Young's modulus vs. polymer concentration and BAPN concentration (log standard deviation = 0.127, $R^2 = 0.90$). The Young's

modulus increases with increasing polymer concentration and BAPN concentration, though the difference between aerogels made with 25 mol % BAPN and 50 mol % BAPN is very small. This is expected since density also increases as polymer concentration and BAPN concentration are increased, which is illustrated in Figure 3. The number of repeat units has a small though significant second order effect on Young's modulus, with the highest Young's modulus corresponding to a n = 45 also following the increase in density.

The plot in Figure 8c shows the compressive log Young's modulus vs. log density of aerogels in the study. The log Young's modulus typically scales linearly with log density in aerogels synthesized with a similar backbone chemistry[45], the solid lines in the figure are to illustrate the linear trend that is seen in this study as well. Aerogels made with 50 mol % BAPN are not shown in this figure, as they are very similar to aerogels made with 25 mol % BAPN, as observed in Figures 8a and 8b. When density is accounted for, the aerogels derived from 75 mol % BAPN have much lower Young's moduli when compared with aerogels derived from 25 mol % BAPN at the same density. This is due to the increase in flexible linkages. For comparison, aerogels in a previously reported study made using only DMBZ and BPDA in the backbone have a Young's modulus 1.5 times higher than those made using 25 mol % BAPN on a same density basis[45], indicating that the addition of BAPN results in a significant reduction in stiffness. Samples made with a higher concentration of aromatic diamines are stiffer but less dense, while samples made with a concentration of aliphatic diamines have reduction in stiffness but also have higher shrinkage, leading to denser structures. These same trends were seen with aerogels made using BAPx in the previous study. In addition, it was observed previously that BAP10 derived aerogels with a ten-methylene spacer, have lower modulus than BAP4 derived aerogels with a shorter four-methylene spacer, especially at 75 mol % BAPx concentration.[35] Hence, since BAPN has a

branched three-carbon aliphatic spacer, the Young's modulus for BAPN derived aerogels have higher modulus than BAP4 aerogels when density is accounted for, as seen in Figure 8c.

Stress-strain curves from tensile tests for selected formulations of aerogels with 8.5 wt % polymer concentration and varying concentrations of BAPN can be found in Figure S1a in the Supporting Information, along with the Empirical model of tensile Young's modulus vs. polymer concentration, and BAPN concentration (Figure S1b) and a Plot of tensile log Young's modulus vs. log density of aerogels made with BAPN concentrations of 25 and 75 mol % and BAP4 concentrations of 25 and 75 mol % (Figure S1c). These results are very similar to the compression testing results.

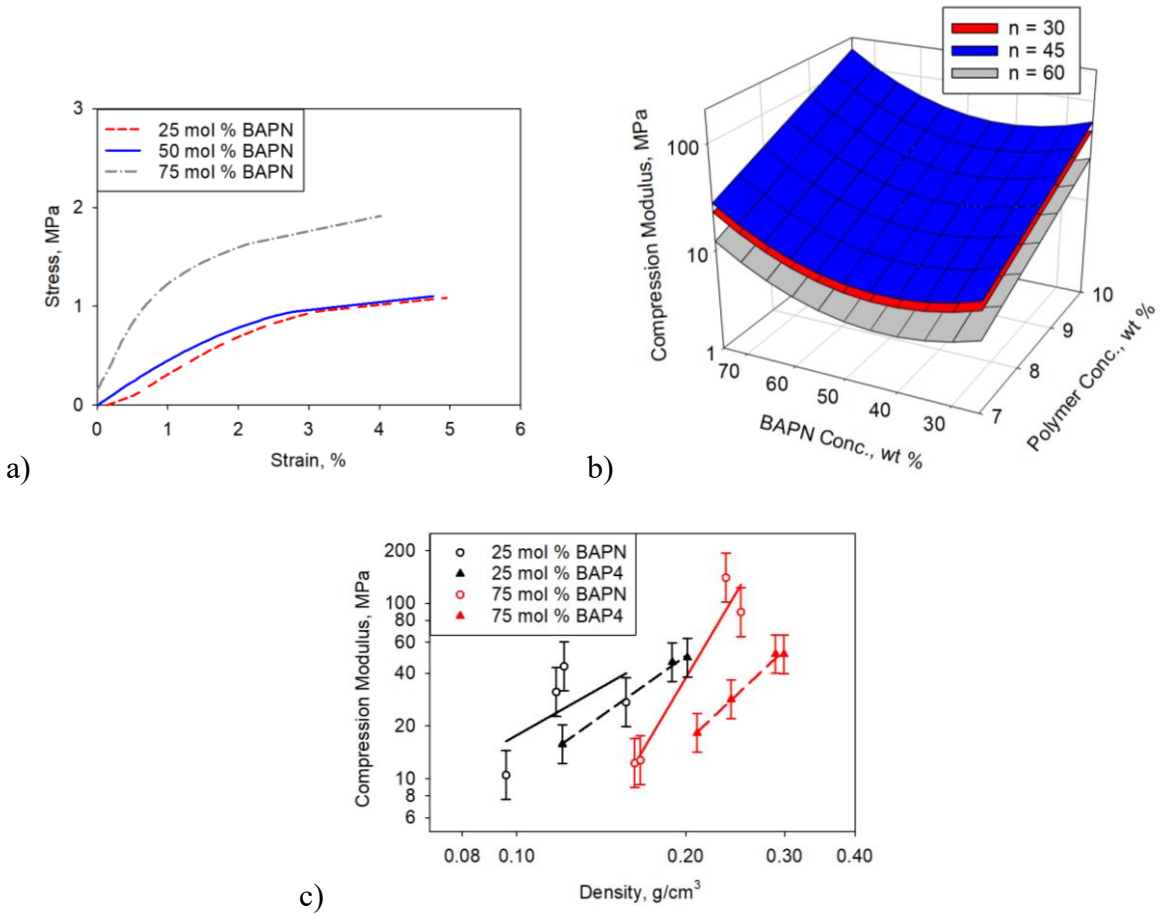

Figure 8. a) Compressive stress-strain curves of aerogels made with 10 wt % polymer concentration and BAPN concentrations of 25, 50, and 75 mol % BAPN b) Empirical model of compressive Young's modulus vs. polymer concentration, and BAPN concentration; c) Plot of compressive log Young's modulus vs. log density of aerogels made with BAPN concentrations of 25 and 75 mol % and BAP4 concentrations of 25 and 75 mol %.

Figure 9a shows the stress-strain curves from three point bending of selected aerogel formulations at 8.5 wt % and varying concentrations of BAPN. The curves show a linear region where elastic deformation is occurring, followed by a plateauing region where yielding and plastic deformation occur. This is then followed by another steep slope, occurring around 13 % strain for samples made with 75 mol % BAPN and around 16 % strain for samples made with 50 and 75 mol % BAPN, where the top of the sample is experiencing tension and the bottom of the sample is

experiencing compression, until finally, the sample experiences flexural failure. The aerogels made using 25 and 50 mol % BAPN have very similar curves, whereas the aerogel made using 75 mol % BAPN reaches higher stress when tested to the same level of strain.

The empirical model for three - point bend Young's modulus in Figure 9b (log standard deviation = 0.085, $R^2 = 0.91$) shows that Young's modulus increases with increasing polymer concentration and a slight parabolic effect with increasing BAPN concentration. The number of repeat units only has a small effect on Young's modulus, similar to compression and tensile moduli (Figure S1b). Figure 9c shows the plot of log density vs three – point bend log Young's modulus. Aerogels made using 75 mol % BAPN have a lower Young's modulus when compared to aerogels made with 25 mol % on a same density basis. Again, this is expected since the increase of flexible linkages reduces the stiffness of the aerogel. Additionally, when comparing BAP4 to BAPN, when density is taken into consideration, the Young's modulus values are somewhat higher, which is the same trend seen for compressive and tensile Young's modulus, indicating that BAPN derived aerogels are less flexible than those derived from BAP4.[35]

Figure 9d shows a 2 mm thick aerogel made using 50 mol % BAPN, 7 wt % polymer concentration and n = 30 being bent at a radius of approximately 1 inch. Aerogels made with 25 mol % BAPN have a similar flexibility. Aerogels made with 75 mol % BAPN were less flexible than those derived from lower BAPN concentrations, due to the increase in density leading to the high modulus.

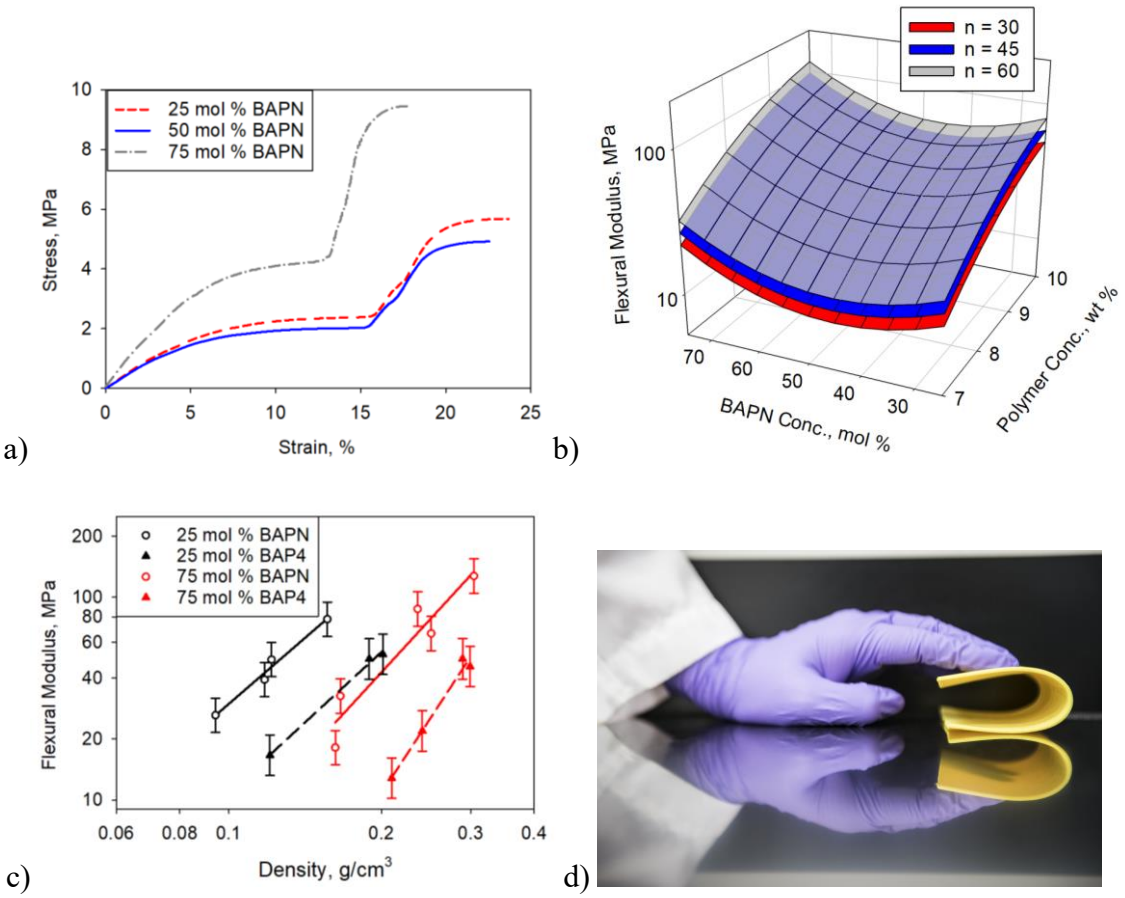

Figure 9. a) Three-point bend stress-strain curves of aerogels made with 8.5 wt % polymer concentration and BAPN concentrations of 25, 50, or 75 mol % BAPN b) Empirical model for three-point bend Young's modulus vs polymer concentration, and BAPN concentration; c) Plot of three-point bend log Young's modulus vs log density of aerogels made with BAPN concentrations of 25 and 75 mol % and BAP4 concentrations of 25 and 75 mol %, d) image showing an approximate 1 inch bend radius of a 2 mm thick aerogel sample made using 7 wt % polymer concentration, 50 mol % BAPN and n = 30.

Though the order of magnitude is the same for compressive, tensile, and flexural Young's modulus, the empirical model for compressive samples do not follow the same trend in regard to n. The empirical compression Young's modulus follows the expected results because a higher n

has a lower cross-link density, so it is expected to have a lower modulus. For the empirical tensile and flexural Young's modulus, the Young's modulus increases with increasing n. This is most likely due to the higher shrinkage and thus higher density that samples with more repeat units experienced. Additionally, the samples used for tensile and flexural testing were thinner than those used for compression. Thinner samples of the same formulations usually have a higher density because the outer surface, which is typically higher in density, makes up a larger portion of the sample.[26]

The aerogels were subjected to water uptake tests to understand the effect of the variables on moisture resistance. The aerogels tested were rectangles, nominally 2.9 cm x 2.0 cm x 0.9 cm in dimension, although since shrinkage varied among the formulations, sample sizes varied. The aerogels were completely immersed in deionized water for 24 hours and weighed before and after testing. The plot for water uptake (log standard deviation = 0.135, R^2 =0.89) is shown in Figure 10. The number of repeat units, n, does not have a significant effect on water uptake above standard error, therefore at some of the same BAPN and polymer concentrations there are multiple points, since n has been ignored. A complete list of formulations and their variables are shown in Table 1. The water uptake range of 0.001 g/cm^2 - 0.01 g/cm^2 corresponds to a weight percent increase range of about 4 - 25 wt %. Aerogels made with 7 wt % polymer concentration and 50 mol % have the smallest water uptake, corresponding to about 4 wt % water, similar to aerogels made using BAP10 in the previous study, and have a considerably lower water uptake than those made with BAP4 and BAP6[35]. In contrast, aerogels made using 10 wt % polymer and 75 mol % BAPN had the highest water uptake, corresponding to 25 wt % water. This is most likely due to pore morphology. Aerogels made with 7 and 10 wt % polymer concentration and higher BAPN concentration (Figure 5a), have very different pore morphology. As seen in the SEM images

(Figure 4), aerogels with 7 wt % polymer concentration have a finer pore structure than aerogels made with 10 wt % polymer concentration. Smaller and finer pores result in increased surface roughness, leading to an increase in hydrophobicity.[48, 49]

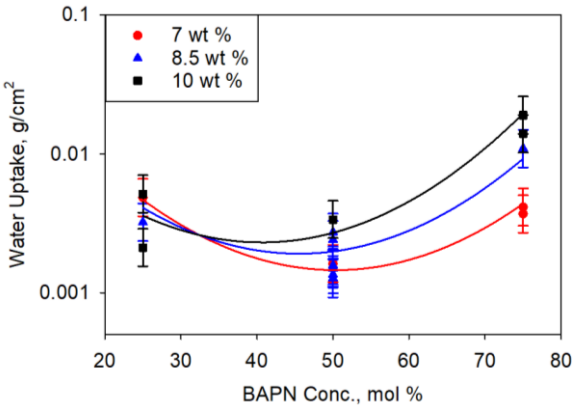

Figure 10. Plot of water uptake vs. polymer concentration.

Aerogels made with 7 wt % polymer concentration, and 50 mol % BAPN have the best combination of properties for use as flexible substrate for lightweight conformal antennas, including the lowest density, smallest dielectric constant, good mechanical properties, flexibility, and good moisture resistance.

Conclusions

Polyimide aerogels are ideal lightweight antenna substrates due to their mechanical robustness, low density and low dielectric constants. Increasing flexibility of the aerogels would allow them to be used as conformal antenna substrates, which would enable new antenna designs that would take up even less space in small aircraft and UAV.[30, 31] A previous study showed that by combining a diamine that has both aliphatic linkages and aromatic rings, BAPx, in conjunction with an all aromatic diamine, DMBZ, that flexible substrates of up to three mm thick can be produced with approximately a 1 inch bend radius.[35] In this study, we demonstrate that by incorporating a neopentyl spacer containing both aliphatic linkages and aromatic rings, BAPN, similar results of

flexibility, low density, low dielectric constant and moisture resistance, comparable to those made from BAP10, can be obtained. Optimal formulations from the study can be made into bendable substrates of up to three mm thick with a bend radius of approximately 1 inch. Properties including density, dielectric constants, water resistance, and mechanical properties were evaluated to understand the effects of the amount of BAPN incorporated into the backbone. Aerogels derived from 50 mol % BAPN and 7 wt % polymer concentration exhibit the lowest density, dielectric constant, and water uptake while still showing good mechanical properties. The optimal aerogel composition in this study has similar moisture resistance with aerogels derived from 25 mol % BAP10, from the previous study, while modulus is somewhat higher.

Supporting Information.

Tensile stress-strain curves, Empirical model of tensile Young's modulus vs. polymer concentration, and BAPN concentration, and Plot of tensile log Young's modulus vs. log density of aerogels made with BAPN concentrations of 25 and 75 mol % and BAP4 concentrations of 25 and 75 mol %

ACKNOWLEDGMENT. We thank the following employees of the Ohio Aerospace Institute: Daniel Scheiman for thermal analysis testing, FTIR, and three- point bend testing. Haiquan Guo for nitrogen sorption measurements, and Linda McCorkle for SEM. We also thank William Brown for compression testing, and Zachary Toom for tensile testing and mechanical testing analysis. We are grateful to the Transformative Aeronautics Concepts Program for funding this work under the Convergent Aeronautic Solutions sub-project: Conformal Lightweight Antenna Systems for Aeronautical Communication Technologies (CLAS-ACT).

References

[1] Pierre, A. C.; Pajonk. G. M. Chemistry of Aerogels and Their Applications. *Chem. Rev.,* **2002,** 102 *(11),* 4243 – 4266.

[2] Husing, N.; Schubert, U. Aerogels- Airy Materials: Chemistry, Structure, and Properties. *Angew. Chem. Int. Ed* **1998**, 37 *(1-2),* 22-45

[3] Gurav, J.; Jung, I.; Park, H.; Kang, E.; Nadargi, D. Silica Aerogel: Synthesis and Applications. *Journal of Nanomaterials,* **2010,** *2010,* 10.1155/2010/409310

[4] Smith, D.M.; Scherer, G.W.; Anderson, J.M. Shrinkage during drying of silica gel. *Journal of Non-Crystalline Solids,* **1995,** *188(3),* 191-206.

[5] Feng, J.; Wang, X.; Jiang, Y.; Du, D.; Feng, J. Study on Thermal Conductivities of Aromatic Polyimide Aerogels. *ACS Appl. Mater. Interfaces,* **2016**, *8(20),* 12992-12996.

[6] Chisca, S.; Sava, I.; Musteata, V.; Bruma, M. Dielectric and Conduction Properties of Polyimide Films. *CAS 2011 Proceedings (2011 International Semiconductor Conference),* Sinaia, Romania **2011,** 253-256

[7] Kravtsova, V.; Umerzakova, M.; Iskakov, R.; Korobova, N. Electrical Properties of Fluoro-Containing Alicyclic Polyimides. *J. Chem. Chem. Eng.* **2015,** *9,* 31-37.

[8] Othman, M. B.; Ming, N. A. S.; Akil, H. M. Ahmad, Z. Dependence of the Dielectric Constant on the Fluorine Content and Porosity of Polyimides. *J. Appl. Polym. Sci.* **2011,** *121,* 3192 – 3200.

[9] Meador, M. A. B.; McMillon, E.; Sandberg, A.; Barrios, E.; Wilmoth, N. G.; Mueller, C. H.; Miranda, F. A. Dielectric and Other Properties of Polyimide Aerogels Containing Fluorinated Blocks. *ACS Appl. Mater. Interfaces* **2014**, *6,* 6062-6068

[10] Smith, D. M.; Anderson, J.; Cho, C. C.; Gnade, B. E. Preparation of low-density xerogels at ambient pressure for low K dielectrics. **1995**, *371*, 261-266.

[11] Meador, M. A. B.; Wright, S.; Sandberg, A.; Nguyen, B. N.; Van Keuls, F. W.; Mueller, C. H.; Rodríguez-Solís, R.; Miranda, F. A. Low Dielectric Polyimide Aerogels as Substrates for Lightweight Patch Antennas. *ACS Appl. Mater. Interfaces* **2012**, *4*, 6346-6353.

[12] Nguyen, B. N.; Meador, M. A. B.; Tousley, M. E.; Shronkwiler, B.; McCorkle, L.; Scheiman, D. A.; Palczer, A. Tailoring Elastic Properties of Silica Aerogels Cross-Linked with Polystyrene. *ACS Appl. Mater. Interfaces* **2009,** *1(3)*, 621-630.

[13] Nguyen, B. N.; Meador, M. A. B.; Medoro, A.; Arendt, V.; Randall, J.; McCorkle, L.; Shonkwiler, B. Elastic Behavior of Methyltrimethoxysilane Based Aerogels Reinforced with Tri-Isocyanate. *ACS Appl. Mater. Interfaces* **2010,** *2(5)*, 1430-1443.

[14] Mandal, C.; Donthula, S.; Soni, R.; Bertino, M.; Sotiriou-Leventis, C.; Leventis, N. Light Scattering and Haze in TMOS-co-APTES Silica Aerogels. *J. Sol-Gel Sci. and Technol.* **2019**, *90(1)*, 127-139.

[15] Lindquist, D. A.; Borek, T. T.; Kramer, S. J.; Narula, C. K.; Johnston, G.; Schaeffer, R.; Smith, D.; Paine, R. T. Formation and Pore Structure of Boron Nitride Aerogels. *Journal of the American Ceramic Society* **1990**, *73(3)*, 757-760.

[16] Nguyen, V. L.; Zera, E.; Perolo, A.; Campostrini, R.; Li, W.; Soraru, G. D. Synthesis and Characterization of Polymer-Derived SiCN Aerogel. *Journal of the European Ceramic Society* **2015**, *35(12)*, 3295-3302.

[17] Wang, L.; Feng, J.; Jiang, Y.; Li, L.; Feng, J. Elastic Methyltrimethoxysilane Based Silica Aerogels Reinforced with Polyvinylmethyldimethoxysilane. *RSC Adv.* **2019**, *9(19)*, 10948-10957.

[18] Leventis, N.; Sotiriou – Leventis, C.; Zhang, G.; Rawashdeh, A. M. Nanoengineering Strong Silica Aerogels. *ACS Nano Letters,* **2002,** *2(9),* 957 – 960.

[19] Al-Muhtaseb, S. A.; Ritter, J. A. Preparation and Properties of Resorcinol-Formaldehyde Organic and Carbon Gels. *Adv. Mater*. **2003**, *15*, 101−114.

[20] Nguyen, B. N.; Cudjoe, E.; Douglas, A.; Scheiman, D.; McCorkle, L.; Meador, M. A. B.; Rowan, S. J. Polyimide Cellulose Nanocrystal Composite Aerogels. *Macromolecules* **2016**, *49*, 1692−1703.

[21] Shang, K.; Yang, J.; Cao, Z.; Liao, W.; Wang, Y.; Schiraldi, D. A. Novel Polymer Aerogel toward High Dimensional Stability, Mechanical Property, and Fire Safety. *ACS Applied Materials & Interfaces* **2017**, *9(27)*, 22985-22993.

[22] Williams, J. C.; Meador, M. A. B.; McCorkle, L.; Mueller, C.; Wilmoth, N. Synthesis and Properties of Step-Growth Polyamide Aerogels Cross-Linked with Triacid Chlorides. *Chem. Mater.* **2014**, *26*, 4163-4171.

[23] Guo, H.; Meador, M. A. B.; McCorkle, L. S.; Scheiman, D. A.; McCrone, J. D.; Wilkewitz, B. Poly(Maleic Anhydride) Cross-Linked Polyimide Aerogels: Synthesis and Properties. *RCS Adv.* **2016**, *6*, 26055-26065.

[24] Leventis, N.; Sotiriou- Leventis, C.; Mohite, D.; Larimore, Z.; Mang, J.; Churu, G.; Lu, H. Polyimide Aerogels by Ring – Opening Metathesis Polymerization (ROMP). *ACS Chem. Mater.* **2011,** *23(8),* 2250-2261.

[25] Sroog, C.E.; Endrey, A. L.; Abramo, S. V.; Berr, C. E.; Edwards, W. M.; Olivier, K. L. Aromatic Polypyromellitimides from Aromatic Polyamic Acids. *J. Polym. Sci., Part A*, **1965**, *3*, 1373 – 1390.

[26] Guo, H.; Meador, M. A. B.; McCorkle, L.; Quade, D. J.; Guo, J.; Hamilton, B.; Cakmak, M. Tailoring Properties of Cross-Linked Polyimide Aerogels for Better Moisture Resistance, Flexibility, and Strength. *ACS Appl. Mater. Interfaces* **2012,** *4*, 5422- 5429.

[27] Gonzalez, F. J.; Ashley, C.S.; Clem, P. G.; Boreman, G. D. Antenna – coupled microbolometer arrays with Aerogel Thermal Isolation, *Infrared Physics and Technology*, **2004,** *45(1),* 47 – 51.

[28] Hrubesh, L.W.; Keene, L. E.; Latorre, V.R. Dielectric Properties of Aerogels. *J. Mater. Res.* **1993**, *8*, 1736−1741.

[29] Meador, M. A. B.; Miranda, F. A. Design and Development of Aerogel-Based Antennas for Aerospace Applications: A Final Report to the NARI Seeding. NASA/TM- 2014-218346.

[30] Callus, P. J. Conformal Load-Bearing Antenna Structure for Australian Defense Force Aircraft. Defense Science and Technology Report; DSTO-TR-1963; file number 2006/1151925.

[31] Leflour, G.; Calnibalosky, C.; Jaquet, H. Reduction of Time and Costs for Antennas Integration through Computational Electro-magnetism. *Proceedings from NATO RTO-AVT Symposium on Reduction of Military Vehicle Acquisition Time and Cost through Advanced Modeling and Virtual Simulation*, Paris, France, April 22-25, **2002**; 59-1—59-10.

[32] Meador, M. A. B.; Malow, E. J.; Silva, R.; Wright, S.; Quade, D.; Vivod, S. L.; Gou, H.; Guo, J.; Cakmak, M. Mechanically Strong, Flexible Polyimide Aerogels Cross-Linked with Aromatic Triamine. *ACS Appl. Mater. Interfaces* **2012,** *4(2),* 536-544.

[33] Amutha, N.; Tharakan, S. A.; Sarojadevi, M. Synthesis and Characterization of New Soluble Polyimides Based on Pyridine Unit with Flexible Linkages. *High Perform. Polym*. **2015**, *27(8),* 979-989.

[34] Lenhardt, J.; Kim, S.; Worsley, M.; Leif, R.; Campbell, P.; Baumann, T.; Satcher, J. ROMP crosslinkers for the preparation of aliphatic aerogels. *Journal of Non-Crystalline Solids* **2015**, *408*, 98-101

[35] Pantoja, M.; Boynton, N.; Cavicchi, K. A.; Dosa, B.; Cashman, J. L.; Meador, M. A. B. Increased Flexibility in Polyimide Aerogels using Aliphatic Spaces in the Polymer Backbone. *ACS Appl. Mater. Interfaces* **2019,** *11*, 9425-9437.

[36] Chidambareswarapattar, C.; McCarver, P.; Luo, H.; Lu, H.; Sotiriou – Leventis, C.; Leventis, N. Fractal Multiscale Nanoporous Polyurethanes: Flexible to Extremely Rigid Aerogels from Multifunctional Small Molecules. *ACS Chem. Mater.* **2013,** *25*, 3205 – 3224.

[37] Bang, A.; Buback, C.; Sotiriou – Leventis, C.; Leventis, N. Flexible Aerogels from Hyperbranched Polyurethanes: Probing the Role of Molecular Rigidity with Poly(Urethane Acrylates) Versus Poly(Urethane Norbornenes). *ACS Chem. Mater* **2014,** *26*, 6979 – 6993.

[38] Donthula, S.; Mandal, C.; Leventis, T.; Schisler, J.; Saeed, A. M.; Sotiriou – Leventis, C.; Leventis, N. Shape Memory Superelastic Poly(isocyanurate – urethane) Aerogels (PIR – PUR) for Deployable Panels and Biomimetic Applications. *ACS Chem. Mater.* **2017,** *29*, 4461 – 4477.

[39] Shinko, A.; Jana, S. C.; Meador, M. A. Crosslinked polyurea – *co* – polyurethane aerogels with hierarchical structures and low stiffness. *Journal of Non-Crystalline Solids* **2018,** *487*, 19 – 27.

[40] Nguyen, B. N.; Meador, M. A. B.; Scheiman, D.; McCorkle, L. Polyimide Aerogels Using Triisocyanate as Cross-linker, **2017**, *9 (32)*, 27313-27321

[41] Janezic, M.D. Nondestructive Relative Permittivity and Loss Tangent Measurements Using a Split- Cylinder Resonator. *Ph.D. Thesis, University of Colorado at Boulder,* **2003.**

[42] Janezic, M. D.; Kuester, E. F.; Baker – Jarvis, J. Broadband Complex Permittivity Measures of Dielectric Substrates using a Split-Cylinder Resonator. *IEEE MTT-S International Microwave Symposium Digest,* **2004,** 1817 – 1820.

[43] Martínez-Richa, A.; Vera-Graziano, R. A Solid-State NMR Study of Aromatic Polyimides Based on 4,4'-Diaminotriphenylmethane. *J. Appl. Polym. Sci*. **1998**, *70*, 1053-1064.

[44] Cheng, . Z. D.; Chalmers, T. M.; Gu, Y.; Yoon, Y.; Harris, F. W. Relaxation processes and Molecular Motion in a New Semicrystalline Polyimide. *Macromol. Chem. Phys.* **1995**, *196 (5)*, 1439-1451.

[45] Meador, M. A. B.; Aleman, C. R.; Hanson, K; Ramirez, N.; Vivod, S. L.; Wilmoth, N.; McCorkle, L. Polyimide Aerogels with Amide Cross-links: A Low Cost Alternative for Mechanically Strong Polymer Aerogels. *ACS Appl. Mater. Interfaces* **2015,** *7,* 1240-1249.

[46] Brunauer, S.; Emmet, P.H.; Teller, E. Adsorption of Gases in Multimolecular Layers. *J. Am. Chem. Soc.* **1938**, *60*, 309 -319.

[47] Cheng, S. Z. D.; Mittleman, M. L.; Janimak, J. J.; Shen, D.; Chalmers, T. M.; Lien, H.; Tso, C. C.; Gabori, P. A.; Harris, F. W. Crystal Structure, Crystallization Kinetics and Morphology of a New Polyimide, *Polymer International* **1992,** *29,* 201 – 208.

[48] Cassie, A. B. D.; Baxter, S. Wettability of Porous Surfaces. *Trans. Faraday Soc.*, **1944**, *40*, 546 – 551.

[49] Zheng, Q.; Lu, C. Size Effects of Surface Roughness to Superhydrophobiticity. *Procedia IUTAM*, **2014,** *10*, 462 – 475.